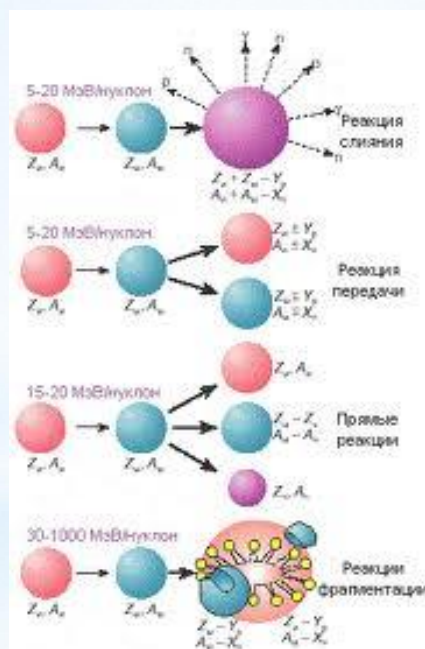


# Application of the Theory of Open Quantum Systems to Nuclear Physics Problems

## З.Каноков

“New aspects of the Hadron and Astro/Nuclear Physics”  
National University of Uzbekistan, Tashkent, November 5-10, 2018



# INTRODUCTION

There are many works devoted to development of the formalism for describing the statistical and dynamic behavior of open systems [1], including those done in Dubna [2]. This formalism is used in nuclear physics to describe fusion, quasifission, multinucleon transfer in heavy-ion reactions, and fission reactions [3]. Interest in stochastic methods appreciably grew in nuclear physics after the discovery of deep-inelastic heavy-ion collisions [4] and a considerable increase in the experimental data on nuclear fission

[1] **A. O. Caldeira and A. J. Leggett**, Physica A 121, 587 (1983); Ann. Phys. 149, 374 (1983); Phys. Rev. Lett. 46, 211 (1981), Phys. Rev. Lett. 48, 1571 (1982). **G. Lindblad**, Commun. Math. Phys. 48, 119 (1976); Rep. Math. Phys. 10, 393 (1976).

[2] **G. G. Adamian, N. V. Antonenko, and W. Scheid**, Nucl. Phys. A 645, 376 (1999).; **Z. Kanokov, Yu. V. Palchikov, G. G. Adamian, N. V. Antonenko, W. Scheid**, Phys. Rev. E 71, 016121 (2005); **Yu. V. Palchikov, Z. Kanokov, G. G. Adamian, N. V. Antonenko, and W. Scheid**, Phys. Rev. E 71, 016122 (2005); **Sh. A. Kalandarov, Z. Kanokov, G. G. Adamian, and N. V. Antonenko**, Phys. Rev. E 74, 011118 (2006); **Sh. A. Kalandarov, Z. Kanokov, G. G. Adamian, and N. V. Antonenko**, Phys. Rev. E 75, 031115 (2007).

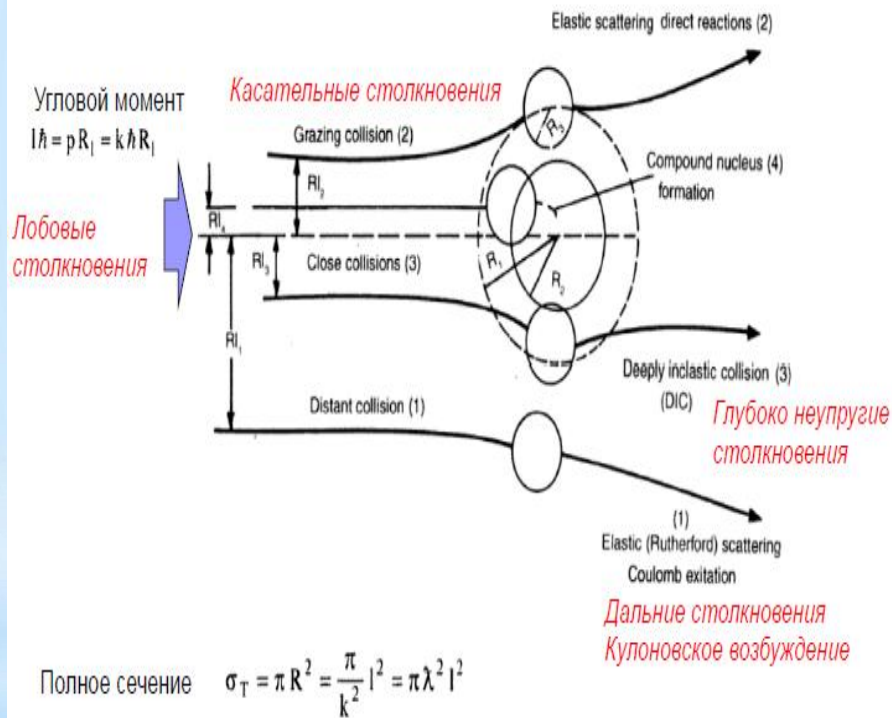
[3] **P. Fröbrich**, Phys. Rep. 116, 337 (1984). ; **G. D. Adeev, I. I. Gonchar**, Fiz. Elem. Chastits At. Yadra 19, 1229 (1988); **G. D. Adeev**, Fiz. Elem. Chastits At. Yadra 23, 1572 (1992). **I. I. Gonchar**, Fiz. Elem. Chastits At. Yadra 23, 932 (1995).; **G. D. Adeev, A. V. Karpov, P. N. Nadtochii, and D. V. Vanin**, Fiz. Elem. Chastits At. Yadra 36, 731 (2005) ; **G. G. Adamian, A. K. Nasirov, N. V. Antonenko, and R. V. Jolos**, Phys. Part. Nucl. 25, 583 (1994)

[4] **V. V. Volkov**, Phys. Rep. 44, 93 (1978); **W. U. Schröder and J. R. Huizenga**, (Plenum Press, New York, 1984), Vol. 2, p. 115.; **V. V. Volkov**, (Plenum Press, New York, 1989), Vol. 8, p. 255.

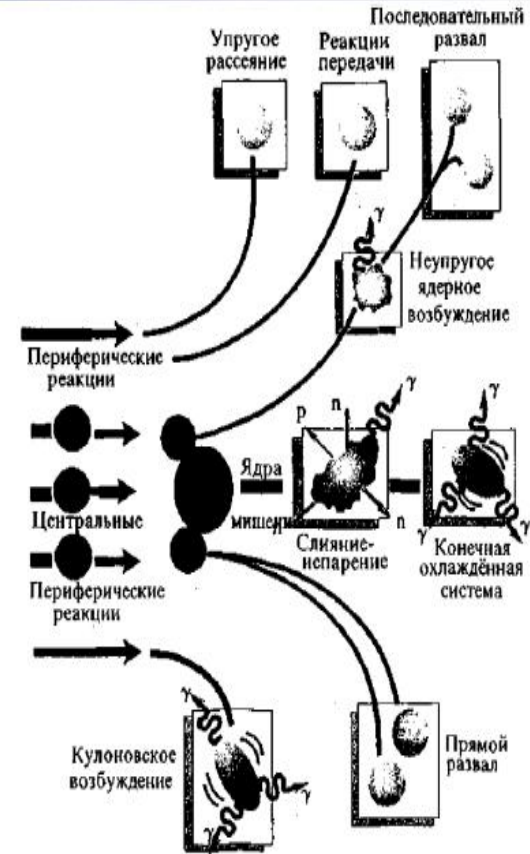
# HEAVY-ION COLLISIONS

## Возможные механизмы взаимодействия иона с ядром

Классификация реакций тяжёлых ионов с ядрами основана на параметре столкновения



Упругое рассеяние чаще происходит при краевых соударениях



Схематическое представление различных реакций с тяжёлыми ионами

## GENERALIZED NON-MARKOVIAN QUANTUM LANGEVIN EQUATIONS

In [R. V. Jolos, S. P. Ivanova, and V. V. Ivanov, *Yad. Fiz.* **40**, 117 (1984); S. P. Ivanova and R. V. Jolos, *Nucl. Phys. A* **530**, 232 (1991).], the quantum Hamiltonian was constructed for nuclear systems, which is explicitly dependent on the collective coordinate  $\mathbf{q}$ , canonically conjugate collective momentum  $\mathbf{p}$ , and internal degrees of freedom

$$H = H_c + H_b + H_{cb}$$

$$H_c = p \frac{1}{2\mu(q)} p + U(q)$$

$$H_b = \sum_{\nu} \hbar \omega_{\nu} b^{\dagger} b \quad H_{cb} = \sum_{\nu} V_{\nu}(q)(b_{\nu}^{\dagger} + b_{\nu}) + i \sum_{\nu} G_{\nu}(q, p)(b_{\nu}^{\dagger} - b_{\nu})$$

$$[b_{\nu}, b_{\nu'}^{\dagger}] = \delta_{\nu\nu'}$$

$$\dot{q}(t) = \frac{1}{2} \{ \tilde{\mu}^{-1}(q), p \}_+ - \frac{1}{2} \int_0^t d\tau \{ K_{GV}(t, \tau), \dot{q}(\tau) \}_+ + \frac{1}{2} \int_0^t d\tau \{ K_{GG}(t, \tau), \dot{p}(\tau) \}_+ + F_q(t)$$

$$\dot{p}(t) = -H_{c,q}(q, p) - \frac{1}{2} \int_0^t d\tau \{ K_{VV}(t, \tau), \dot{q}(\tau) \}_+ + \frac{1}{2} \int_0^t d\tau \{ K_{VG}(t, \tau), \dot{p}(\tau) \}_+ + F_p(t)$$

$$q(t) = A_t q(0) + B_t p(0) + \int_0^t d\tau [G_\tau F_q(t-\tau) + \tilde{G}_\tau F_p(t-\tau)],$$

$$p(t) = M_t q(0) + N_t p(0) + \int_0^t d\tau [L_\tau F_p(t-\tau) + \tilde{L}_\tau F_q(t-\tau)],$$

$$A_t = L^{-1} \left[ \frac{s(1 + K_{GV}(s))(1 - K_{VG}(s)) + (\tilde{\mu}^{-1} + sK_{GG}(s))K_{VV}(s)}{d(s)} \right]$$

$$N_t = L^{-1} \left[ \frac{s(1 - K_{VG}(s))(1 + K_{GV}(s)) + (\tilde{\delta} + sK_{VV}(s))K_{GG}(s)}{d(s)} \right],$$

$$B_t = L^{-1} \left[ \frac{\tilde{\mu}^{-1}(1 - K_{VG}(s))}{d(s)} \right]$$

$$M_t = -L^{-1} \left[ \frac{\tilde{\delta}(1 + K_{GV}(s))}{d(s)} \right]$$

$$\tilde{C}_t = L^{-1} \left[ \frac{\tilde{\mu}^{-1} + sK_{GG}(s)}{d(s)} \right]$$

$$C_t = L^{-1} \left[ \frac{s(1 - K_{VG}(s))}{d(s)} \right]$$

$$L_t = L^{-1} \left[ \frac{s(1 + K_{GV}(s))}{d(s)} \right]$$

$$\tilde{L}_t = -L^{-1} \left[ \frac{\tilde{\delta} + sK_{VV}(s)}{d(s)} \right]$$

$$d(s) \equiv s^2(1 + K_{GV}(s))(1 - K_{VG}(s)) + (\tilde{\delta} + sK_{VV}(s))(1/\tilde{\mu} + sK_{GG}(s)) = 0.$$

$$\sum_v \phi_{qp}^v(t, t') \frac{th[\frac{\hbar\omega_v}{2T}]}{\hbar\omega_v} = K_{GV}(t, t')$$

## TRANSPORT COEFFICIENTS

Using explicit time dependences of  $\mathbf{p}$  and  $\mathbf{q}$ , we obtain their main characteristics, i.e., the mean values and (first moments)

$$\frac{d}{dt} \langle q(t) \rangle = -\lambda_q(t) \langle q(t) \rangle + \frac{1}{m(t)} \langle p(t) \rangle$$

$$\frac{d}{dt} \langle p(t) \rangle = -\xi_q(t) \langle q(t) \rangle + \lambda_p(t) \langle p(t) \rangle$$

$$\dot{\sigma}_{qq}(t) = -2\lambda_q(t)\sigma_{qq}(t) + \frac{2}{m(t)}\sigma_{pq}(t) + 2D_{qq}(t)$$

$$\dot{\sigma}_{pp}(t) = -2\lambda_p(t)\sigma_{pp}(t) - 2\xi_q(t)\sigma_{pq}(t) + 2D_{pp}(t)$$

$$\dot{\sigma}_{pq}(t) = -[\lambda_p(t) + \lambda_q(t)]\sigma_{pq}(t) - \xi_q(t)\sigma_{qq}(t) + \frac{1}{m(t)}\sigma_{pp}(t) + 2D_{pq}(t)$$

## RELATION TO THE DIFFUSION EQUATIONS

$$\begin{aligned}\dot{\rho} = & -\frac{i}{\hbar}[\tilde{H}_c, \rho] + i\frac{\lambda_q(t)}{2\hbar}[p, \{q, \rho\}_+] - \\ & -i\frac{\lambda_p(t)}{2\hbar}[q, \{p, \rho\}_+] - \frac{D_{qq}(t)}{\hbar^2}[p, [p, \rho]] - \\ & -\frac{D_{pp}(t)}{\hbar^2}[q, [q, \rho]] + \frac{D_{pq}(t)}{\hbar^2}([p, [q, \rho]] + [q, [p, \rho]])\end{aligned}$$

$$\begin{aligned} \dot{W} = & -\frac{p}{m(t)} \frac{\partial W}{\partial q} + \xi(t) \frac{\partial W}{\partial p} + \\ & + \lambda_p(t) \frac{\partial(pW)}{\partial q} + \lambda_q(t) \frac{\partial(qW)}{\partial p} + \\ & + D_{qq}(t) \frac{\partial^2 W}{\partial q^2} + D_{pp}(t) \frac{\partial^2 W}{\partial p^2} + 2D_{pq}(t) \frac{\partial^2 W}{\partial q \partial p} \end{aligned}$$

$$D_{pp} D_{qq} - D_{qp}^2 \geq \frac{\hbar^2}{4} (\lambda_q + \lambda_p)^2$$

$$\sigma_{pp} \sigma_{qq} - \sigma_{qp}^2 \geq \frac{\hbar^2}{4}$$



$$H_{cb} = q \sum_{\nu} \alpha_{\nu} (b_{\nu}^{+} + b_{\nu}) + ip \sum_{\nu} g_{\nu} (b_{\nu}^{+} - b_{\nu})$$

$$H_{cb} = \lambda^{1/2} \sum_{\nu} \Gamma_{\nu} (a^{+}(t) + a(t)) (b_{\nu}^{+} + b_{\nu}) = \sqrt{\frac{2\lambda\mu\omega}{\hbar}} q \sum_{\nu} \Gamma_{\nu} (b_{\nu}^{+} + b_{\nu})$$

$$\dot{q}(t) = \frac{p(t)}{\mu}$$

$$\dot{p}(t) = -\tilde{\delta}q(t) - k^2 \int_0^t d\tau K(t-\tau) \dot{q}(\tau) + kF(t)$$

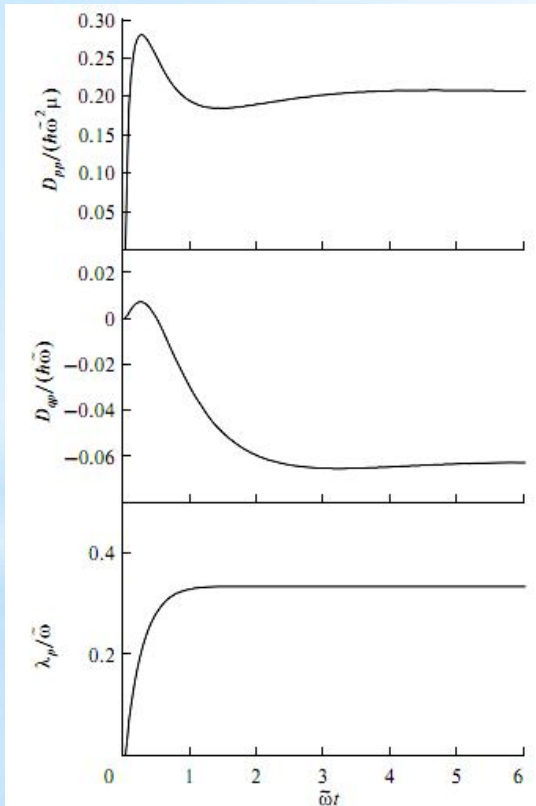


Fig. 1. Time dependences of the diffusion and frictions coefficients calculated at  $\hbar\tilde{\omega} = 3$  MeV,  $\mu = 50m_0$ , and  $T/(\hbar\tilde{\omega}) = 0.033$ . Here  $\hbar\lambda_p(\infty) = 1$  MeV.

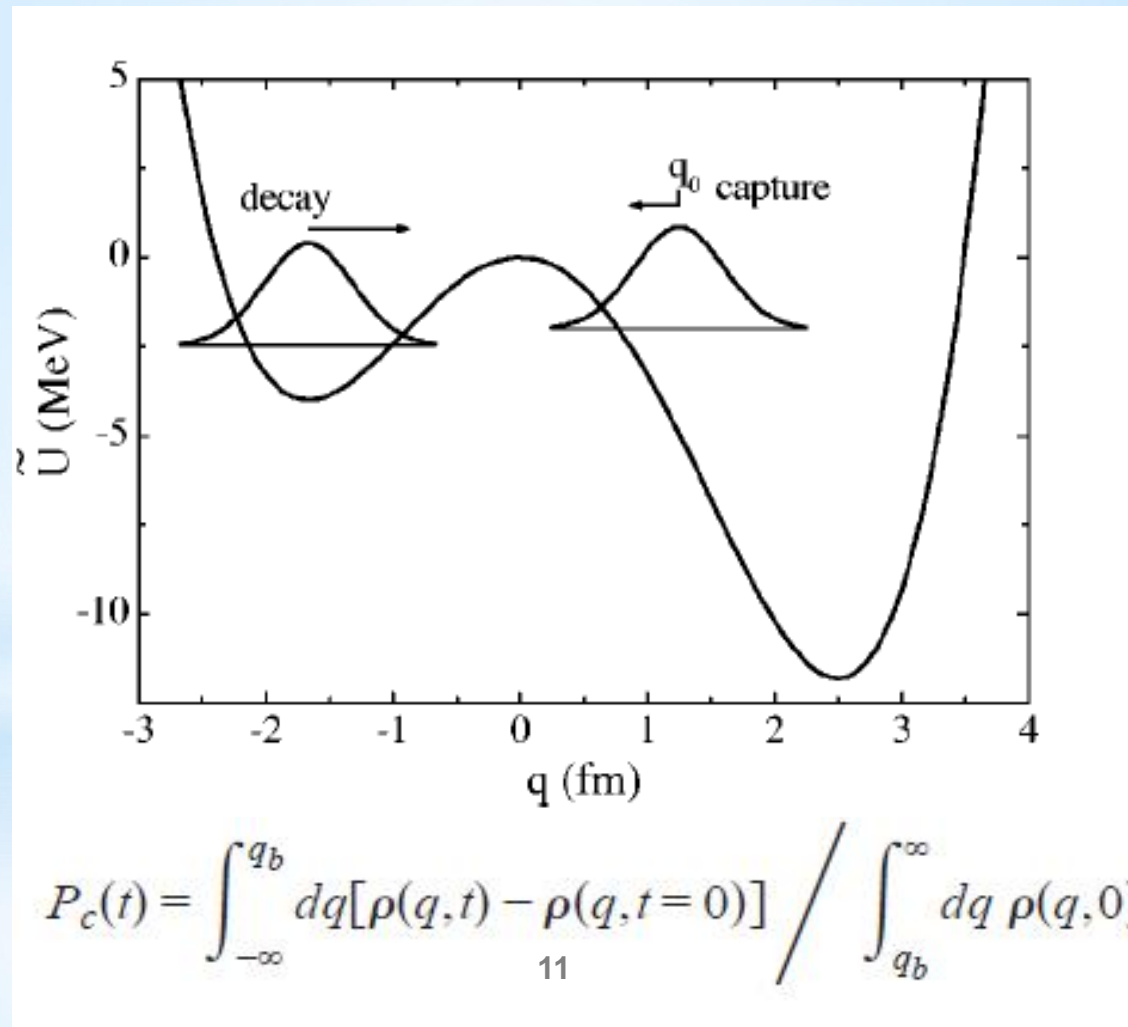
In the limits of low and high temperatures the asymptotic ( $t \gg t' > 0$ ) symmetrized correlation function

$$\sigma_{q_t q_{t'}} = \frac{\lambda \gamma^2}{2\pi \hbar \omega \mu} \int_0^\infty d\omega_0 \frac{\omega_0 [2n_{\omega_0} + 1] \cos(\omega_0 [t - t'])}{[s_i + i\omega_0]^2 [s_2 + i\omega_0]^2},$$

$$\sigma_{p_t p_{t'}}^{as} (T \rightarrow 0) \rightarrow -\frac{\hbar g_0 \tilde{\mu}^2 \mu^2 \omega^4}{(\mu \omega^2 - \tilde{\mu} \xi_0^2)^2} \frac{1}{(t - t')^2}$$

$$\tilde{U}(q) = \frac{6q_R V_L}{q_L^2 (2q_R - q_L)} q^2 - \frac{4(q_L + q_R) V_L}{q_L^3 (q_L - 2q_R)} q^3 - \frac{3V_L}{q_L^3 (2q_R - q_L)} q^4 =$$

$$= -3.24q^2 - 0.43q^3 + 0.39q^4$$



# CAPTURE OF THE PROJECTILE NUCLEUS BY THE TARGET NUCLEUS

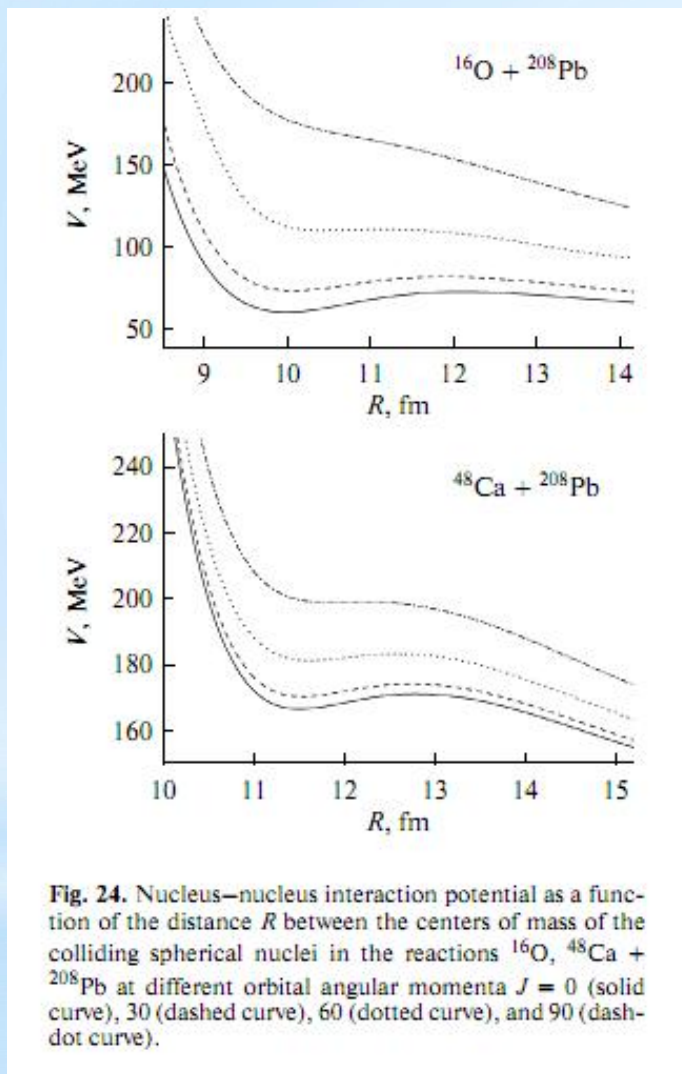


Fig. 24. Nucleus–nucleus interaction potential as a function of the distance  $R$  between the centers of mass of the colliding spherical nuclei in the reactions  $^{16}\text{O}$ ,  $^{48}\text{Ca}$  +  $^{208}\text{Pb}$  at different orbital angular momenta  $J = 0$  (solid curve), 30 (dashed curve), 60 (dotted curve), and 90 (dash-dot curve).

$$V(R, J) = V_{\text{nuc}}(R) + V_{\text{Coul}}(R) + V_{\text{rot}}(R, J),$$

$$V_{\text{nuc}} = \int \rho_1(\mathbf{r}_1) \rho_2(\mathbf{R} - \mathbf{r}_2) F(\mathbf{r}_1 - \mathbf{r}_2) d\mathbf{r}_1 d\mathbf{r}_2$$

$$V_{\text{Coul}} = e^2 \int \frac{\rho_1^z(\mathbf{r}_1) \rho_2^z(\mathbf{R} - \mathbf{r}_2)}{|\mathbf{r}_1 - \mathbf{r}_2|} d\mathbf{r}_1 d\mathbf{r}_2$$

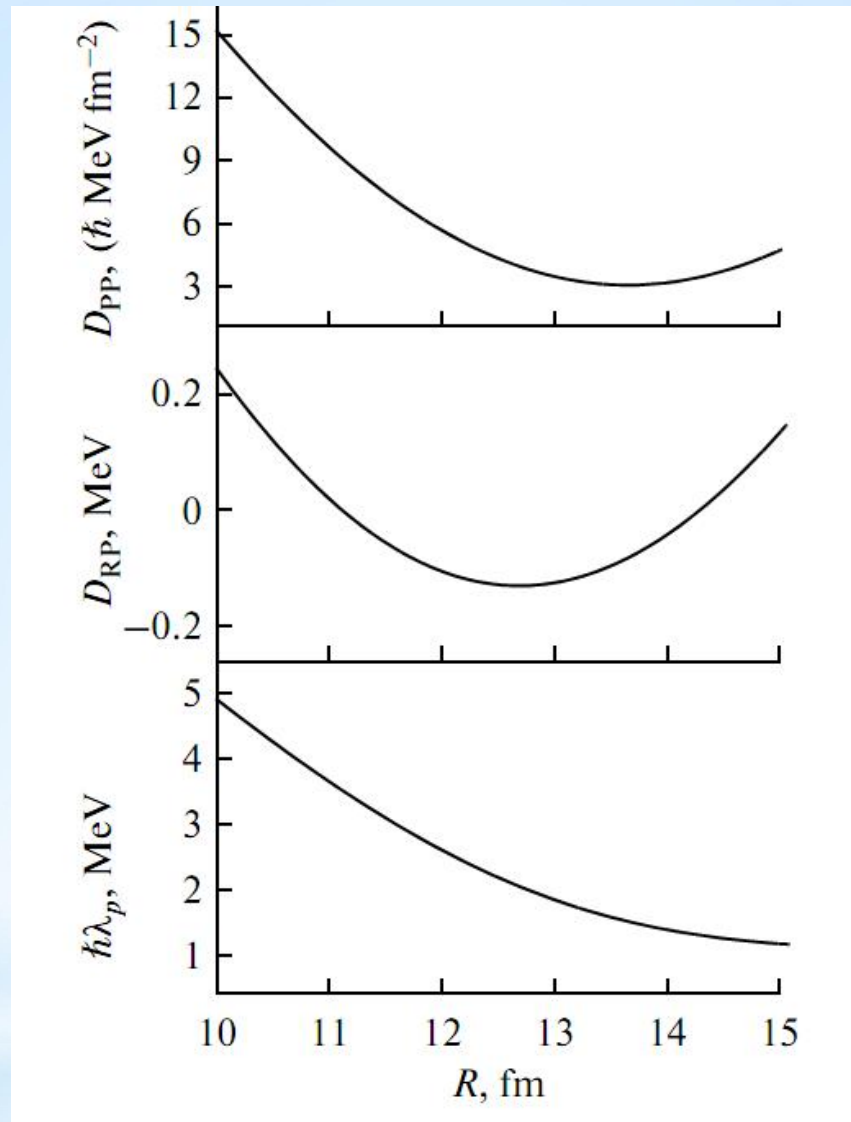
$$V_{\text{rot}} = \frac{\hbar^2 J(J+1)}{2\mu R^2}$$

$$P(t = \tau, E_{\text{c.m.}}, L, \Omega_p, \Omega_T) = \frac{\int_{-\infty}^0 \rho(R, t = \tau) dR}{\int_0^{\infty} \rho(R, t = 0) dR}.$$

$$\sigma_c(E_{\text{c.m.}}, J) = \pi \lambda^2 (2J + 1) P_{\text{cap}}(E_{\text{c.m.}}, J),$$

$$\sigma_c(E_{\text{c.m.}}) = \sum_J \sigma_c(E_{\text{c.m.}}, J)$$

$$= \pi \lambda^2 \sum_J (2J + 1) P_{\text{cap}}(E_{\text{c.m.}}, J),$$



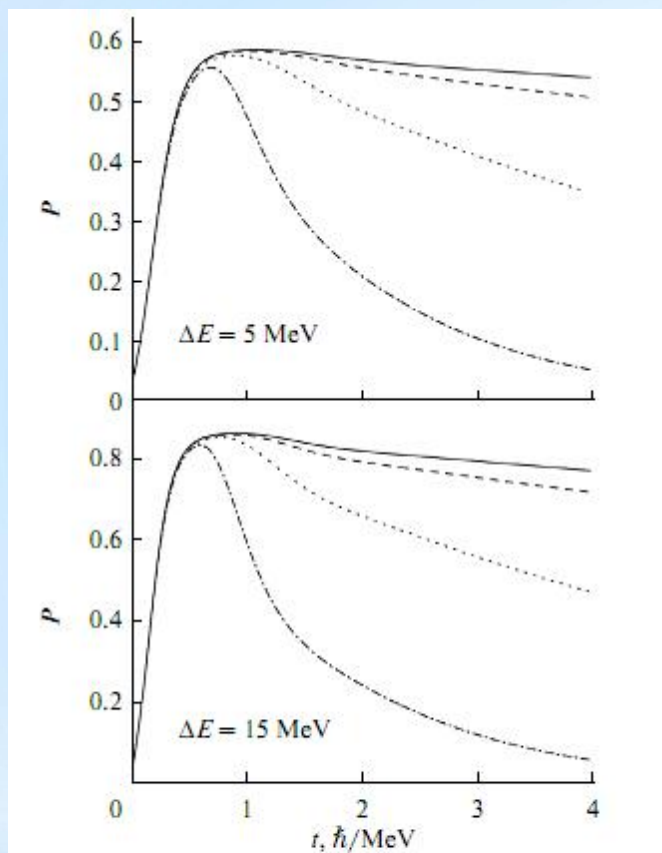


**Fig. 26.** Time dependence of the capture probability  $P$  at the collision energies  $\Delta E = E_{c.m.} - V(R = R_b, J) = 5$  MeV and 15 MeV in the  $^{48}\text{Ca} + ^{208}\text{Pb}$  reaction. The energy is measured from the Coulomb barrier at the given angular momentum  $J$ . The different curves correspond to different angular momenta:  $J = 0$  (solid curve), 30 (dashed curve), 60 (dotted curve), and 90 (dash-dot curve). The parameter  $\alpha$  is chosen from the condition  $\hbar\lambda_p(R_b) = 2$  MeV.

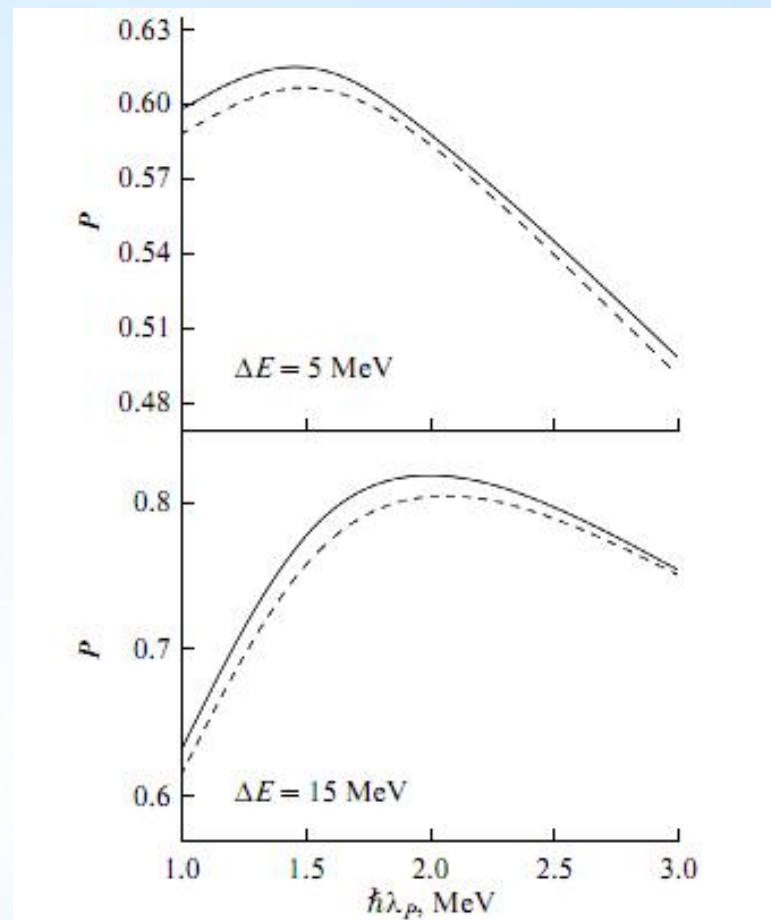


**Fig. 28.** Capture probability  $P$  as a function of the friction coefficient  $\hbar\lambda_p(R_b)$  in the reaction  $^{48}\text{Ca} + ^{208}\text{Pb}$  at the given energies,  $\hbar\gamma = 12$  MeV (solid curve) and 20 MeV (dashed curve).

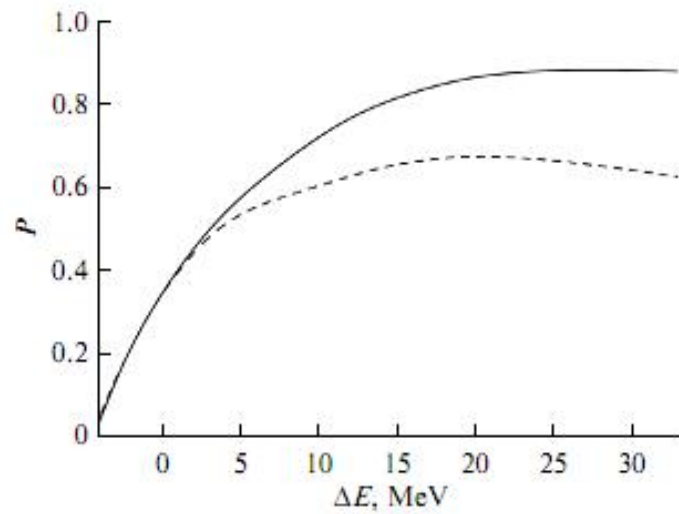


**Fig. 27.** Capture probability  $P$  as a function of the collision energy  $\Delta E = E_{\text{c.m.}} - V(R = R_b, J)$  measured from the Coulomb barrier height at  $J = 0$  (solid curve) and 60 (dashed curve) in the  $^{48}\text{Ca} + ^{208}\text{Pb}$  reaction.

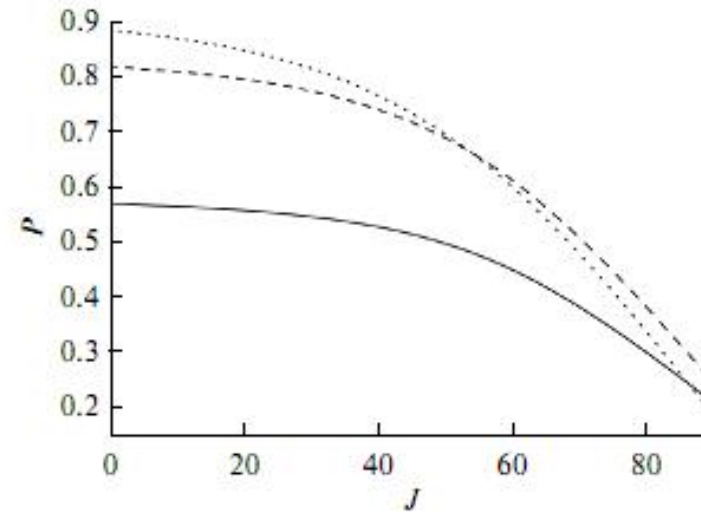


**Fig. 29.** Capture probability  $P$  as a function of the orbital angular momentum  $J$  at  $\Delta E(0) = 5$  MeV (solid curve), 15 MeV (dashed curve), and 30 MeV (dotted curve) in the  $^{48}\text{Ca} + ^{208}\text{Pb}$  reaction. The energy  $\Delta E(0)$  is measured from the Coulomb barrier at  $J = 0$ . Here  $\hbar\lambda_p = 2$  MeV.

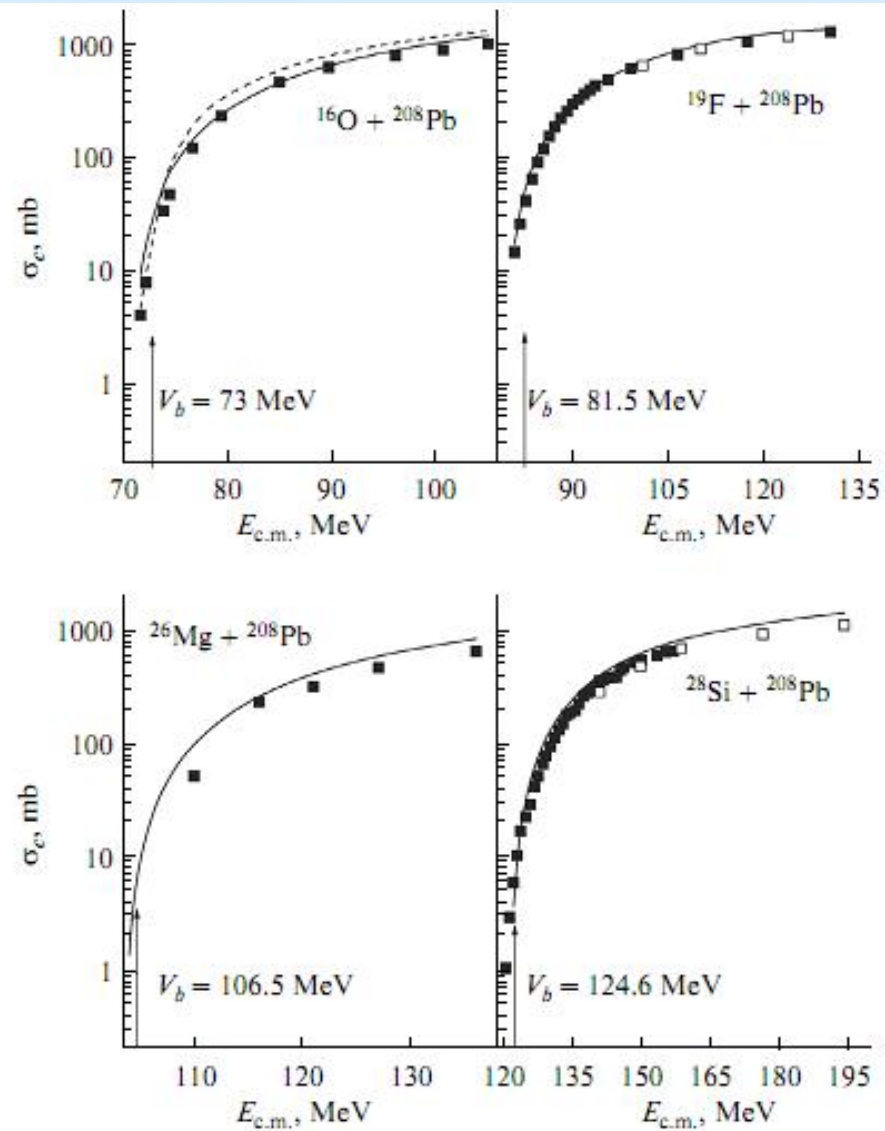


**Fig. 30.** Calculated capture cross sections (solid curves) for the given reactions. The experimental data are from [58] for the  $^{16}\text{O} + ^{208}\text{Pb}$  reaction, from [59] (filled symbols) and [60] (open symbols) for the  $^{19}\text{F} + ^{208}\text{Pb}$  reaction, from [61] for the  $^{26}\text{Mg} + ^{208}\text{Pb}$  reaction, and from [62] (filled symbols) and [60] (open symbols) for the  $^{28}\text{Si} + ^{208}\text{Pb}$  reaction. The dashed curve is the capture cross sections for the  $^{16}\text{O} + ^{208}\text{Pb}$  reaction calculated using Wong formula (116).



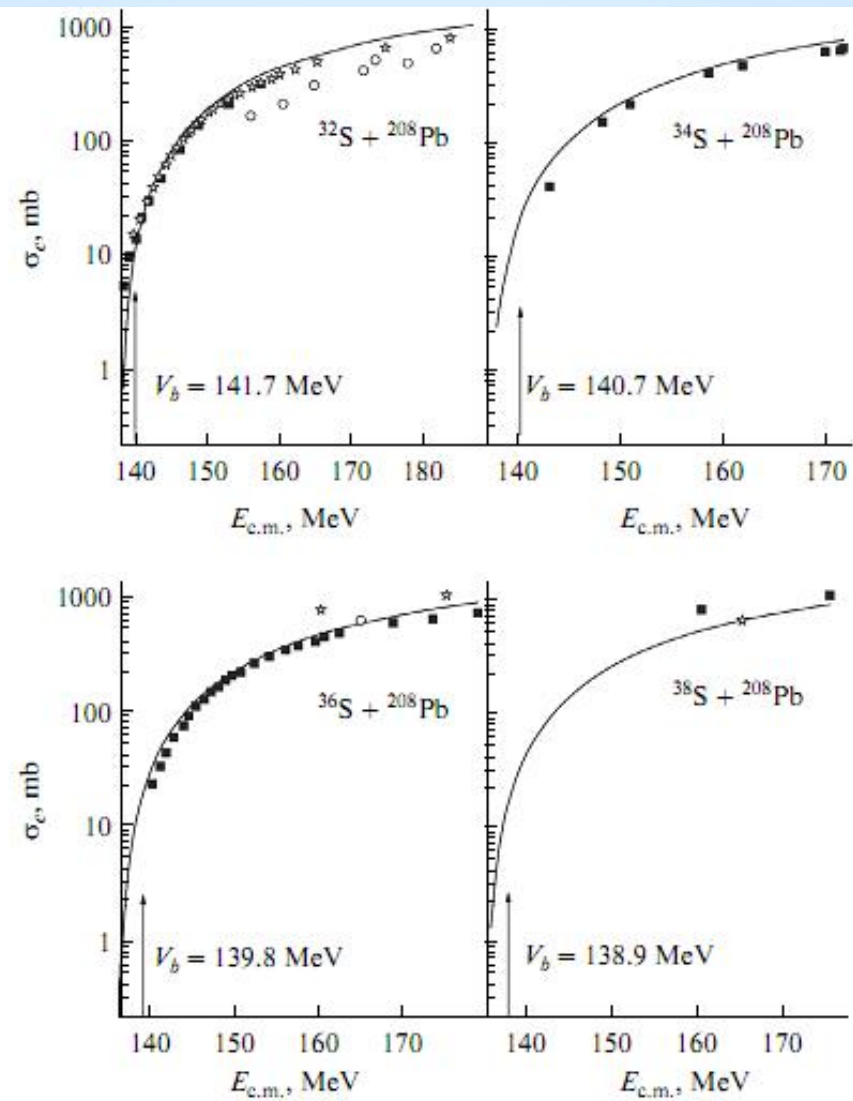


**Fig. 31.** Calculated capture cross sections (solid curves) for the given reactions. The experimental data are from [63] (filled symbols), [64] (stars), and [65] (circles) for the reaction  $^{32}\text{S} + ^{208}\text{Pb}$ , from [64] for the reaction  $^{34}\text{S} + ^{208}\text{Pb}$ , from [64] (filled symbols) and [65] (stars and open symbols) for the reaction  $^{36}\text{S} + ^{208}\text{Pb}$ , and from [65] (filled squares and stars) for the reaction  $^{38}\text{S} + ^{208}\text{Pb}$ .

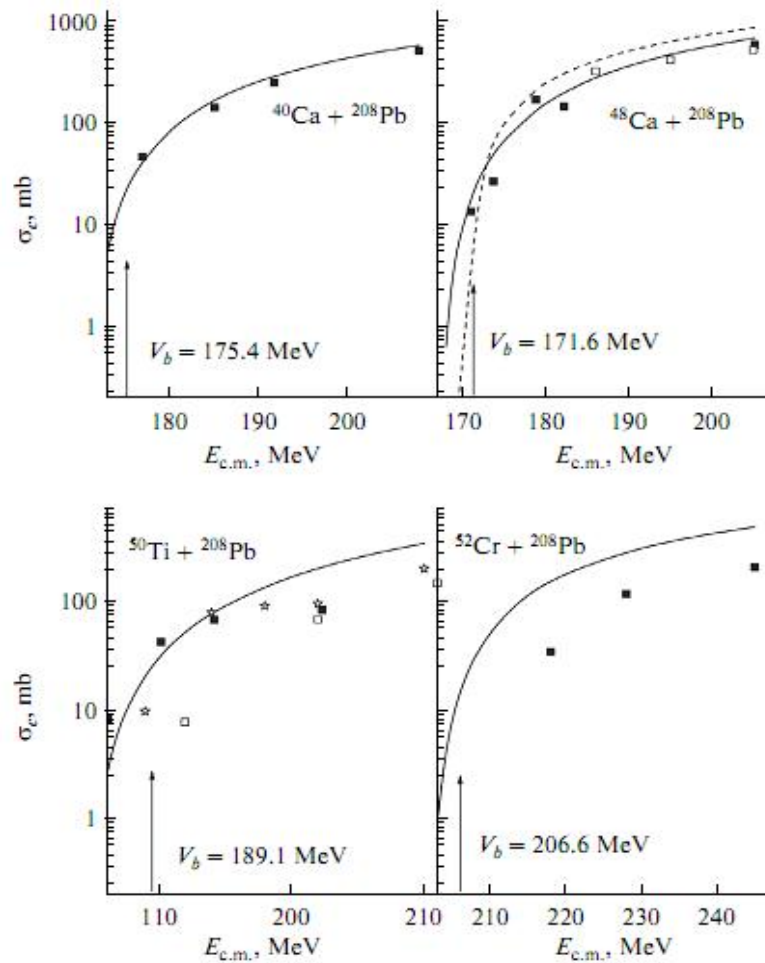


**Fig. 32.** Calculated capture cross sections (solid curves) for the given reactions. The experimental data are from [66] for the  $^{40}\text{Ca} + ^{208}\text{Pb}$  reaction, from [66] (filled symbols) and [67] (open symbols) for the  $^{48}\text{Ca} + ^{208}\text{Pb}$  reaction, from [68] (filled symbols), [61] (open symbols), and [69] (stars) for the  $^{50}\text{Ti} + ^{208}\text{Pb}$  reaction, and from [61] for the  $^{52}\text{Cr} + ^{208}\text{Pb}$  reaction. The dashed curve shows the capture cross sections for the  $^{48}\text{Ca} + ^{208}\text{Pb}$  reaction calculated using Wong formula (116).

$$\sigma_c(E_{c.m.}) = \frac{\hbar\omega_b R_b^2}{2E_{c.m.}} \ln \left[ 1 + \exp \left( \frac{2\pi(E_{c.m.} - V_b)}{\hbar\omega_b} \right) \right],$$

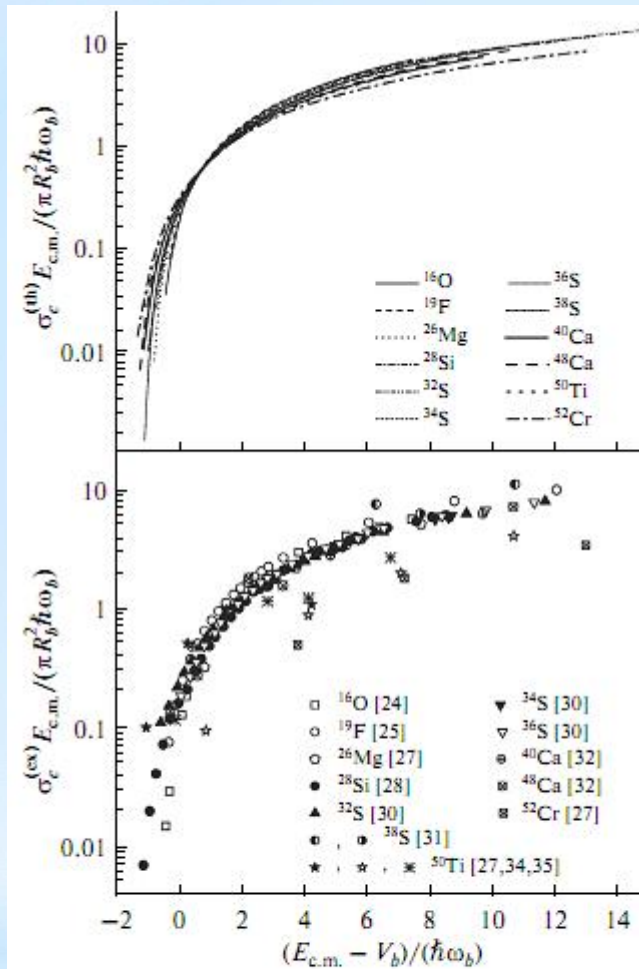
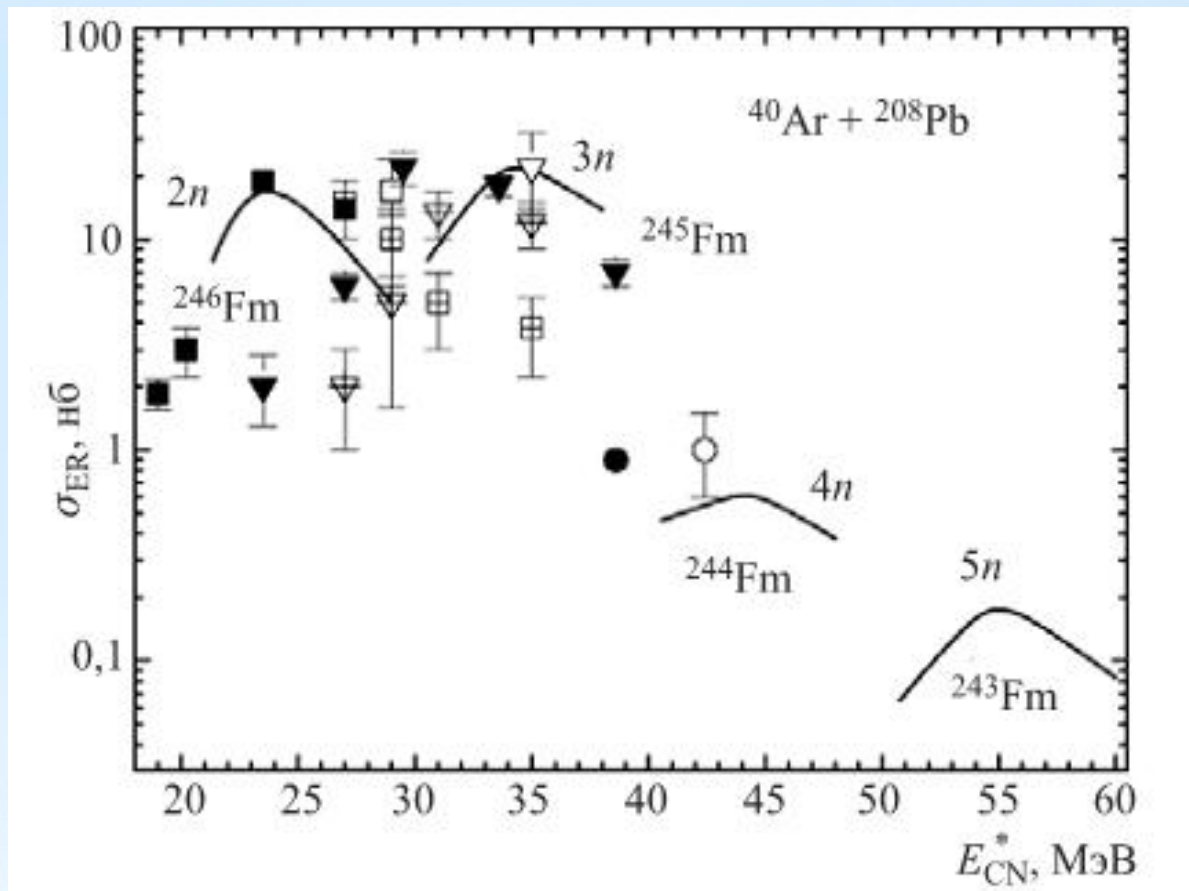


Fig. 33. Dependence of the calculated (top) and experimental (bottom)  $\sigma_c E_{c.m.} / (\pi R_b^2 \hbar \omega_b)$  on  $(E_{c.m.} - V_b) / (\hbar \omega_b)$  for the reactions with the  $^{208}\text{Pb}$  target and the given projectiles. Here  $V_b = V(R = R_b, J = 0)$ .



Рассчитанные сечения функций возбуждения и испарительных остатков для указанных

*хп*-испарительных каналов в реакции  $^{40}\text{Ar} + ^{208}\text{Pb}$

## CONCLUSIONS

- A system of nonlinear Langevin equations is derived within the microscopic approach in the limit of the general coupling between the collective and internal (boson or fermion) subsystems.
- These equations of motion for the collective subsystem satisfy the quantum fluctuation–dissipation relations and the uncertainty relation.
- A new method for obtaining explicitly time-dependent transport coefficients is developed on the basis of the non-Markovian Langevin equations.
- The predicted power-law decay of the oscillator correlation functions in the limit of low temperatures and large times can be the subject of experimental investigation.
- The analytical formulas obtained in this work can be used for describing the fluctuation–dissipation dynamics of nuclear processes with complex potentials. The developed approach helps to describe lifetimes of metastable systems, transition processes, and decoherence in quantum systems.
- We were the first to use the reduced density matrix formalism for describing the capture of the projectile nucleus by the target nucleus. Good agreement between the theoretical calculations and the available experimental data was obtained for the cross sections of capture in the  $^{16}\text{O}$ ,  $^{19}\text{F}$ ,  $^{26}\text{Mg}$ ,  $^{28}\text{Si}$ ,  $^{32,34,36,38}\text{S}$ ,  $^{40,48}\text{Ca}$ ,  $^{50}\text{Ti}$  +  $^{208}\text{Pb}$  reactions. This justifies further use of the proposed capture cross section calculation method.

спасибо

за внимание !



$$\frac{dR(t)}{dt} = \frac{P(t)}{\tilde{\mu}} + \frac{1}{2} \int_{t_0}^t dt' \{K_{PR}(t, t'), \dot{R}(t')\}_+ + \frac{1}{2} \int_{t_0}^t dt' \{K_{PP}(t, t'), \dot{P}(t')\}_+ + F_R(t)$$

$$\frac{dP(t)}{dt} = -\frac{\partial U(R(t))}{\partial R(t)} - \frac{1}{2} \int_{t_0}^t dt' \{K_{RR}(t, t'), \dot{R}(t')\}_+ - \frac{1}{2} \int_{t_0}^t dt' \{K_{RP}(t, t'), \dot{P}(t')\}_+ - F_P(t)$$

$$\dot{E}(t) = - \left[ 2\lambda_p(t) + \frac{\dot{m}(t)}{m(t)} \right] \frac{\sigma_{pp}(t) + \langle p(t) \rangle^2}{2m(t)} - [2\lambda_q(t)\xi(t) + \dot{\xi}(t)] \frac{\sigma_{qq}(t) + \langle q(t) \rangle^2}{2} + \frac{D_{pp}(t)}{m(t)} + \xi(t)D_{qq}(t)$$

Из этого уравнения видно, что для гармонического осциллятора скорость диссипации растёт с  $\mu$  и убывает с ростом  $D_{pp}(t)$  и  $D_{qq}(t)$ .